Effect of apodization on the retrieval of geophysical parameters from Fourier-transform spectrometers

Umberto Amato, Daniela De Canditiis, and Carmine Serio

The problem of the effect of apodization on the retrieval of geophysical parameters from infrared radiances recorded by Fourier transform spectrometers has been analytically and numerically addressed. Exploiting a matrix representation of apodization, we first derive a general analytical expression for the apodized covariance matrix and then show that apodization, when properly applied, has no effect on retrievals. The methodology has been applied to investigate the effect of Gaussian apodization on the Infrared Atmospheric Sounding Interferometer currently under development at the laboratories of the French Space Agency.

OCIS codes: 300.0300, 010.1290, 070.6020, 120.0280.

1. Introduction

Apodization is the name by which Fourier spectroscopists refer to the windowing operation in Fourier analysis. It is the mathematical tool devised to alleviate the effect of the so-called truncation error. Truncation error arises as a consequence of the finite extent of a time or spatial function. Because of the natural and obvious restrictions of experimental equipment, information is available only for a given recording time T, so that the function stops abruptly at T. The Fourier transform of this clipped function shows ringing on the spectral features.

If one asks a Fourier mathematician to explain apodization, the reply would likely be that the tool is used to improve the convergence properties of the Fourier series when only a finite amount of a time or spatial function is available. On the other hand, to the same question a Fourier spectroscopist would likely reply that apodization is needed to make the spectrum recorded with a Fourier-transform spectrometer (FTS) look like a spectrum recorded with a grating spectrometer. Despite the two seemingly different replies, both answers underline the common requirement of a spectral response function narrower than the one intrinsic to a FTS. However, apodization, being a convolution, implies smoothing of the original function. Thus, if we try to achieve too much smoothing, e.g., to have a spectrum that looks perfectly like the corresponding grating spectrometer product, we may sacrifice significant frequency information.

In this paper we address the effect of apodization on the retrieval of geophysical parameters from FTS radiances. The problem is now receiving enormous attention in the scientific community because of the many FTS space missions that are planned in the framework of next-generation meteorological and climatological satellites. This work, indeed, arises in the framework of the Infrared Atmospheric Sounding Interferometer (IASI) project, although the methodology and the results outlined apply to any FTS.

The IASI is part of the core payload of the European Polar System of the European Organization for the Exploitation of Meteorological Satellites. The IASI is currently under development at the laboratories of the French National Space Agency (Centre National d'Etudes Spatiales).

The instrument is a spectrometer interferometer (Michelson design) with a spectral coverage from 3.6 to 15.5 μm and a spectral sampling interval of 0.25 cm^{-1}. It is being developed to meet the specifications issued by the World Meteorological Organization (i.e., temperature with an average error of 1 K; humidity with an average error of 10%; vertical resolution of 1 km, at least in the lower troposphere).

U. Amato is with the Istituto per Applicazioni della Matematica, Consiglio Nazionale delle Ricerche, Napoli, Italy. D. De Canditiis is with the Dipartimento di Matematica, Universita di Napoli "Federico II," Napoli, Italy. C. Serio is with the Dipartimento di Ingegneria e Fisica Ambientale, Università della Basilicata, via della Tecnica 3, 85100 Potenza, Italy. C. Serio is also with the Istituto Nazionale di Fisica della Materia, Genoa, Italy.

Received 29 July 1997; revised manuscript received 23 March 1998.

0003-6935/98/276537-07$15.00/0

More details about the IASI and its expected accuracy can be found, e.g., in Refs. 1 and 2.

Apodization may be used to solve particular technical problems that occur frequently in spectroscopic applications. Among many others, it can alleviate the problem of negative transmittances, which may arise when convolving line-by-line synthetic radiances with the intrinsic FTS spectral response function. This problem occurs because of the many sidelobes that characterize the intrinsic instrumental spectral response function of a FTS and may become acute when dealing with the development of a fast forward model. Another advantage is that apodization may reduce the range of spectral smearing caused by observing at a finite resolution.

The following two main problems, then, arise:

1. How does the covariance matrix of the radiances transform under apodization?
2. How will apodization affect retrieval of geophysical parameters?

This paper will address specifically the two questions above. In particular,

1. an analytical representation of the apodization matrix will be presented, and then a general analytical expression for the covariance matrix of the apodized products will be derived; and
2. a formal mathematical proof that the set of Rodgers's equations (e.g., Ref. 3) to solve nonlinear inverse problems are invariant under apodization will be provided.

The two results above will be obtained in a general mathematical context and will apply to any FTS, not only to the IASI. In particular, result 1 works for any apodizing function, and result 2 can be easily extended to any linear inverse method, e.g., Tikhonov regularization (Ref. 4), or nonlinear inverse methods that incorporate the Newton–Raphson algorithm in their mathematical machinery, e.g., the Levenberg–Marquardt algorithm (Ref. 5).

The mathematical material in this paper has been previously presented in a series of meetings (e.g., Ref. 6) and has not been published yet. This material is presented here on a more systematic basis. We hope that it may provide an analytical methodological basis, with emphasis on the retrieval problem, for users interested in data processing and analysis of FTS signals.

An excellent treatment of windowing in Fourier analysis and its impact on the Fourier transform can be found in the original work of Harris (Ref. 7). Special analytical apodizing functions for a FTS are discussed, e.g., in Refs. 8 and 9.

This paper is organized as follows. Section 2 is devoted to the mathematical theory: Subsection 2.A deals with basic facts, Subsection 2.B presents the analytical representation of the apodization matrix, and Subsection 2.C is devoted to the assessment of the effect of apodization on retrievals. In Section 3 the mathematical theory is used to address specific points of interest for the IASI system. Conclusions are drawn in Section 4.

2. Mathematical Theory

A. Basic Equations and Definitions

To fix the idea, we shall assume to be dealing with a FTS spectrometer that measures the upwelling infrared emission spectrum of the Earth from space. However, the same conclusions apply to any of the various operational modes of a FTS. Our analysis will be performed mainly in the wave-number or spectral domain, since users typically have access to the spectrum rather than to its Fourier transform, i.e., the interferogram. The latter is the quantity directly measured by a FTS.

The emission spectrum $S(\sigma)$ (σ being the wave number) of a given source is physically defined in the interval $[0, \infty]$. However, according to the Shannon–Wittaker sampling theorem (e.g., Ref. 10), only band-limited functions can be effectively sampled without loss of information. In practice, the band-limited property is achieved by suitable optical filtering, so that the spectrum $S(\sigma)$ may be mathematically represented by the band-limited function:

$$S(\sigma) = \begin{cases} \text{arbitrary} & \text{for } \sigma_1 \le \sigma \le \sigma_2 \\ 0 & \text{otherwise} \end{cases}. \qquad (1)$$

Furthermore, the auxiliary condition $\sigma_1 = l(\sigma_2 - \sigma_1)$, where l is an integer, must be fulfilled for a proper sampling of the spectrum. To cope with the symmetry of the Fourier transform and for a correct application of the convolution theorem, formal mathematical calculations employ the even function $R_t(\sigma)$, defined in the interval $[-\infty, \infty]$: $R_t(\sigma) = R_t(-\sigma) = S(\sigma)/2$. Note that this definition leaves the total energy unchanged, that is,

$$\int_{-\infty}^{+\infty} R_t(\sigma)\mathrm{d}\sigma = \int_{0}^{+\infty} S(\sigma)\mathrm{d}\sigma.$$

The function (1) is often referred to as the one-sided spectrum, whereas $R_t(\sigma)$ is the two-sided spectrum. The interferogram $C(x)$, which is the function actually sampled by the FTS, is then the Fourier transform of $R_t(\sigma)$:

$$C(x) = \int_{-\infty}^{+\infty} R_t(\sigma)\exp(-i2\pi\sigma x)\mathrm{d}\sigma.$$

Note that $C(x)$ is itself an even function, and x is a spatial coordinate, physically related to the optical path difference of the two light beams that travel in the interferometer.

The relation between the FTS spectrum and the

corresponding infinite-resolution, or true, spectrum is expressed by the superposition integral

$$R(\sigma) = \int_{-\infty}^{+\infty} R_t(\sigma_0) w(\sigma; \sigma_0) \mathrm{d}\sigma_0, \tag{2}$$

where $R(\sigma)$ and $R_t(\sigma)$ are, respectively, the FTS spectrum and the infinite-resolution spectrum, w is the instrumental spectral response function (ISRF), and σ again denotes wave number.

For an ideal FTS, w is the sine cardinal, or sinc, function:

$$w(\sigma) = 2L \frac{\sin(2\pi\sigma L)}{2\pi\sigma L},$$

where L is the maximum optical path difference. It determines the spectral sampling interval $\delta\sigma = (2L)^{-1}$ (e.g., Ref. 11). The ISRF for an ideal FTS does not change its functional form as σ moves along the wave-number axis. In addition, it is shift invariant, i.e., $w(\sigma; \sigma_0) = w(\sigma - \sigma_0)$, so that Eq. (2) is a convolution. However, because of the phenomenon of self-apodization, an instrumental effect that is mainly due to the finite extent of the field of view of the spectrometer, it is possible that w is less than ideal and not shift invariant, which justifies our notation $w(\sigma; \sigma_0)$. Relation (2) is the signal model for a FTS and is the starting point to compute synthetic radiances that are needed, e.g., in the inversion step. Once the ISRF for a given FTS is known, synthetic radiances can be computed on the basis of a suitable radiative transfer model, which provides R_t. To model the data, we need to add a noise term on the right-hand side of Eq. (2) that models measurement, processing, and other kinds of error. We have

$$D(\sigma) = R(\sigma) + \varepsilon(\sigma), \tag{3}$$

where the D's are the observations (or data) and $\varepsilon(\sigma)$ is a noise term. For a good FTS spectrometer (e.g., Ref. 11), $\varepsilon(\sigma)$ is nearly Gaussian and largely uncorrelated, i.e., $\langle \varepsilon(\sigma)\varepsilon(\sigma') \rangle = 0$ for $\sigma \neq \sigma'$, with the angle brackets denoting expectation value.

B. Machinery of Apodization

The natural ISRF of a FTS is not particularly appealing, since it is broad and decays slowly to zero. This means that the spectral radiance $R(\sigma)$ at a given wave number σ receives a contribution, through the convolution (2), from a large wave-number interval at the expense of computational speed and efficiency. This problem may become acute when convolving synthetic transmittances and/or radiances, since it may produce negative transmittances/radiances. These negative values are not particularly attractive if we have to use those transmittances to develop fast forward models.

For this reason we may intervene with mathematical windowing to produce a narrower ISRF. In practice, this can be done by convolving Eq. (2) with a suitable further window $g(\sigma)$ to give the apodized radiances $R_a(\sigma)$ (with the subscript a meaning apodized):

$$\begin{aligned} R_a(\sigma) &= \int_{-\infty}^{+\infty} R(\sigma') g(\sigma - \sigma') \mathrm{d}\sigma' \\ &= \int_{-\infty}^{\infty} \int_{-\infty}^{+\infty} R_t(\sigma_0) w(\sigma'; \sigma_0) g(\sigma - \sigma') \mathrm{d}\sigma_0 \mathrm{d}\sigma' \\ &= \int_{-\infty}^{+\infty} R_t(\sigma_0) \mathrm{d}\sigma_0 \int_{-\infty}^{+\infty} w(\sigma'; \sigma_0) g(\sigma - \sigma') \mathrm{d}\sigma' \\ &= \int_{-\infty}^{+\infty} R_t(\sigma_0) f(\sigma; \sigma_0) \mathrm{d}\sigma_0, \end{aligned} \tag{4}$$

where

$$f(\sigma; \sigma_0) = \int_{-\infty}^{+\infty} w(\sigma'; \sigma_0) g(\sigma' - \sigma) \mathrm{d}\sigma'$$

is the apodized instrumental response.

To obtain synthetic radiances, it is preferable first to compute $f(\sigma; \sigma_0)$, since this computation can be done only once, and then to obtain the apodized radiances according to Eq. (4). However, the computation can also be performed in the interferogram domain, where the convolution integral becomes the product of two Fourier transforms.

This last procedure is to be preferred when considering how to compute the convolution integral for the observations:

$$D_a(\sigma) = \int_{-\infty}^{\infty} D(\sigma') g(\sigma - \sigma') \mathrm{d}\sigma'. \tag{5}$$

In this case we have only a limited amount of observations $D(\sigma)$, already convolved with the intrinsic ISRF of the given FTS and sampled at N discrete values of σ. The brute force approximation of the convolution integral (5) with a discrete summation could lead to a large quadrature error. For this reason the operation is more efficiently performed in the interferogram domain. It should be noted that the spectrum, being band limited, has a Fourier transform (its interferogram) that can be exactly described by a finite number of discrete values, so that, by operating in the interferogram domain, we can compute the integral (5), without approximations, with a finite discrete summation. It also important to stress that in Eq. (5) D represents a calibrated spectrum; our procedure cannot merely be extended to raw interferograms. Mathematical apodization works for calibrated spectra or interferograms.

The operation involves the following steps:

1. Compute the Fourier transform $C(k\Delta x)$ of the observations $D(\sigma)$,
2. compute the Fourier transform $G(x)$ of $g(\sigma)$,
3. obtain the product $P(k\Delta x) = C(k\Delta x)G(k\Delta x)$, and

4. obtain the apodized set of radiances by Fourier (inverse) transforming the product $P(k\Delta x)$.

In all steps Δx is the sampling interval in the spatial domain, where $\Delta x = [2(\sigma_2 - \sigma_1)]^{-1}$.

The operations above involve a round trip from the spectral domain to the interferogram domain and back to the spectral domain. The nice thing is that this round trip may be performed with a one-way ticket, since the two ways turn out to be identical. This is a result of the evenness of both interferogram and spectrum, which allows us to use only the one-sided spectrum [see Eq. (1)] and therefore real quantities alone. Let $\mathbf{d}$ be the N vector of unapodized radiances (one-sided radiances); we assume that the radiances are computed, as usual, at the harmonic wave numbers:

$$\sigma_k = \sigma_1 + \frac{\sigma_2 - \sigma_1}{N - 1}(k - 1), \qquad k = 1, \ldots, N,$$

where N is the number of observations. The apodized radiances are given by

$$\mathbf{d}_a = (\mathbf{UGU})\mathbf{d}, \tag{6}$$

where $\mathbf{U}$ is the $N \times N$ matrix defined as

$$U_{ij} = \begin{cases} \dfrac{1}{\sqrt{2(N-1)}} & \text{for } j = 1,\ i = 1, \ldots, N \\ \dfrac{2}{\sqrt{2(N-1)}} \cos\dfrac{\pi(i-1)(j-1)}{N-1} & \text{for } j = 2, \ldots, N-1,\ i = 1, \ldots, N \\ \dfrac{1}{\sqrt{2(N-1)}} \cos[\pi(i-1)] & \text{for } j = N,\ i = 1, \ldots, N \end{cases} \tag{7}$$

and $\mathbf{G}$ is the diagonal matrix whose null elements are the N apodizing weights $G_i := G((i - 1)\Delta x)$, $i = 1, \ldots, N$, with the function G being the Fourier transform of g. From the well-known properties of the Fourier transform, we have $\mathbf{U} = \mathbf{U}^{-1}$.

From Eq. (6) we immediately obtain that the transformation $\mathbf{UGU}$ is singular if and only if $\mathbf{G}$ is. Since $\mathbf{G}$ is a diagonal matrix, the transform will be singular if at least one weight G_i is zero. Furthermore, since according to Eq. (6) apodization involves a linear transformation of the radiances, at best it does not add information. Information may be lost if $\mathbf{G}$ becomes singular (no inverse).

Finally, it is important to realize that because of the additive model (3), the error transforms exactly how the observations do. Thus, if $\mathbf{S}$ is the covariance matrix of the unapodized observations, then the apodized covariance matrix $\mathbf{S}_a$ is

$$\mathbf{S}_a = \mathbf{OSO}^{\mathrm{T}}, \tag{8}$$

with

$$\mathbf{O} = \mathbf{UGU}. \tag{9}$$

Equations (6)–(9) give the formulas, valid for any kind of apodization and any observational covariance matrix, to compute the apodized covariance matrix. Using these relations, we can now easily understand the effect of apodization on the inversion step.

C. Apodization Has No Effect on the Retrievals

Remote sensing of Earth's atmosphere from upwelling infrared radiances is nonlinear. However, inversion procedures typically end up in a linearization method, where the forward model equation

$$\mathbf{d} = \mathbf{F}(\mathbf{v}) \tag{10}$$

is linearized by expanding Eq. (10) as a Taylor series about a guessed value $\mathbf{v}_n$ of the solution. In Eq. (10) $\mathbf{v} = (v_1, \ldots, v_M)$ is the atmospheric state parameter vector, where the M parameters may include temperature profiles and gas constituent profiles as well, $\mathbf{d}$ is the radiance vector, and $\mathbf{F}$ is the forward model function.

Linearization results in the following linear problem:

$$\mathbf{d} - \mathbf{d}_n = \mathbf{K}_n(\mathbf{v}_{n+1} - \mathbf{v}_n), \tag{11}$$

which, by taking account of the error covariance matrix of the observations, $\mathbf{S}$, becomes

$$\mathbf{S}^{-1/2}(\mathbf{d} - \mathbf{d}_n) = \mathbf{S}^{-1/2}\mathbf{K}_n(\mathbf{v}_{n+1} - \mathbf{v}_n), \tag{12}$$

to be solved iteratively on n. In Eqs. (11) and (12), $\mathbf{v}_n$ is the atmospheric state parameter at iteration n, $\mathbf{K}_n = \partial\mathbf{F}/\partial\mathbf{v}$ is the Jacobian matrix computed at $\mathbf{v}_n$, $\mathbf{d}_n$ is the radiance vector corresponding to state vector $\mathbf{v}_n$, and $\mathbf{d}$ is the radiance vector corresponding to the observations; $\mathbf{v}_0$ is a suitable background state whose covariance matrix is $\mathbf{S}_v$.

According to Rodgers (Ref. 3), a popular iterative (regularized) solution of the problem (12) is

$$\mathbf{v}_{n+1} = \mathbf{v}_0 + (\mathbf{S}_v^{-1} + \mathbf{K}_n^{\mathrm{T}}\mathbf{S}^{-1}\mathbf{K}_n)^{-1}\mathbf{K}_n^{\mathrm{T}}\mathbf{S}^{-1}[(\mathbf{d} - \mathbf{d}_n) - \mathbf{K}_n(\mathbf{v}_0 - \mathbf{v}_n)]. \tag{13}$$

We want to show that when the apodization step is applied to the radiances, the solution (13) to the corresponding linear problem does not change. To this end we consider the apodized version of the problem (11),

$$\mathbf{O}(\mathbf{d} - \mathbf{d}_n) = \mathbf{OK}_n(\mathbf{v}_{n+1} - \mathbf{v}_n),$$

so that the corresponding problem, taking account of the error covariance matrix of the apodized variances, $\mathbf{S}_a$, becomes

$$\mathbf{S}_a^{-1/2}\mathbf{O}(\mathbf{d} - \mathbf{d}_n) = \mathbf{S}_a^{-1/2}\mathbf{O}\mathbf{K}_n(\mathbf{v}_{n+1} - \mathbf{v}_n).$$

The Rodgers solution becomes

$$\mathbf{v}_{n+1}^{(a)} = \mathbf{v}_0 + (\mathbf{S}_v^{-1} + \mathbf{K}_{an}^{\mathrm{T}}\mathbf{S}_a^{-1}\mathbf{K}_{an})^{-1}\mathbf{K}_{\mathrm{an}}^{\mathrm{T}}\mathbf{S}_a^{-1}[(\mathbf{d}_a - \mathbf{d}_{an}) - \mathbf{K}_{an}(\mathbf{v}_0 - \mathbf{v}_n)], \quad (14)$$

where $\mathbf{v}_{n+1}^{(a)}$ is the solution expressed in terms of apodized radiances and the subscript a has been added to all the apodized quantities on the right-hand side of the equation. There are two terms in Eqs. (13) and (14) that are affected by apodization. The first one concerns the covariance matrix of the solution,

$$(\mathbf{S}_v^{-1} + \mathbf{K}_{an}^{\mathrm{T}}\mathbf{S}_a^{-1}\mathbf{K}_{an})^{-1}.$$

To show that this term is left unchanged, it suffices to consider the apodized term $\mathbf{K}_{an}^{\mathrm{T}}\mathbf{S}_a^{-1}\mathbf{K}_{an}$. Keeping in mind that the covariance matrix transforms according to Eq. (8), we have

$$\mathbf{K}_{an}^{\mathrm{T}}\mathbf{S}_a^{-1}\mathbf{K}_{an} = (\mathbf{O}\mathbf{K}_n)^{\mathrm{T}}(\mathbf{O}\mathbf{S}\mathbf{O}^{\mathrm{T}})^{-1}\mathbf{O}\mathbf{K}_n = \mathbf{K}_n^{\mathrm{T}}\mathbf{O}^{\mathrm{T}}(\mathbf{O}^{\mathrm{T}})^{-1}\mathbf{S}^{-1}\mathbf{O}^{-1}\mathbf{O}\mathbf{K}_n = \mathbf{K}_n^{\mathrm{T}}\mathbf{S}^{-1}\mathbf{K}_n,$$

provided that $\mathbf{O}$ is not singular, so that

$$(\mathbf{S}_v^{-1} + \mathbf{K}_{an}^{\mathrm{T}}\mathbf{S}_a^{-1}\mathbf{K}_{an})^{-1} = (\mathbf{S}_v^{-1} + \mathbf{K}_n^{\mathrm{T}}\mathbf{S}^{-1}\mathbf{K}_n)^{-1}; \quad (15)$$

that is, the covariance matrix of the solution is left unchanged under apodization. The second term in Eq. (14) that is affected by apodization is

$$\mathbf{K}_{an}^{\mathrm{T}}\mathbf{S}_a^{-1}[(\mathbf{d} - \mathbf{d}_{an}) - \mathbf{K}_{an}(\mathbf{v}_0 - \mathbf{v}_n)],$$

which, when the dependence on the apodizing matrix $\mathbf{O}$ is made explicit, becomes

$$\begin{aligned}\mathbf{K}_{an}^{\mathrm{T}}\mathbf{S}_a^{-1}[(\mathbf{d}_a - \mathbf{d}_{an}) - \mathbf{K}_{an}(\mathbf{v}_0 - \mathbf{v}_n)] &= \mathbf{K}_n^{\mathrm{T}}\mathbf{O}^{\mathrm{T}}(\mathbf{O}^{\mathrm{T}})^{-1}\mathbf{S}^{-1}\mathbf{O}^{-1}\mathbf{O}[(\mathbf{d} - \mathbf{d}_n) - \mathbf{K}_n(\mathbf{v}_0 - \mathbf{v}_n)] \\ &= \mathbf{K}_n^{\mathrm{T}}\mathbf{S}^{-1}[(\mathbf{d} - \mathbf{d}_n) - \mathbf{K}_n(\mathbf{v}_0 - \mathbf{v}_n)]. \quad (16)\end{aligned}$$

Equations (15) and (16) prove our statement that the solution is left unchanged under apodization.

The basic ingredient that makes the proof work is the linearization step that is taken at each iteration [Eq. (12)]; therefore all the methods that rely on the Newton–Raphson procedure, e.g., the Levenberg–Marquardt algorithm (Ref. 5), are not affected by apodization. The invariance of linear inverse problems is trivial.

It is important to note that we need to require the matrix $\mathbf{O}$ to have the inverse, which is the case if $\mathbf{G}$ is not singular. Singularity may occur in case of heavy apodization, which causes the last weights, G_i, to be zero. The matrix $\mathbf{G}$ then has one or more zero rows. Heavy apodization is likely to introduce loss of information in the spectrum. It should be stressed that if $\mathbf{G}$ is singular, then the covariance matrix has no inverse and the retrievals cannot be obtained by the usual tools. In this case we must reduce the set of apodized radiances until the covariance matrix possesses its inverse. In practice, heavy apodization moves the truncation point in the interferogram closer to the origin, and therefore it decreases the maximum path delay L, which inevitably causes a loss of information in the spectral range.

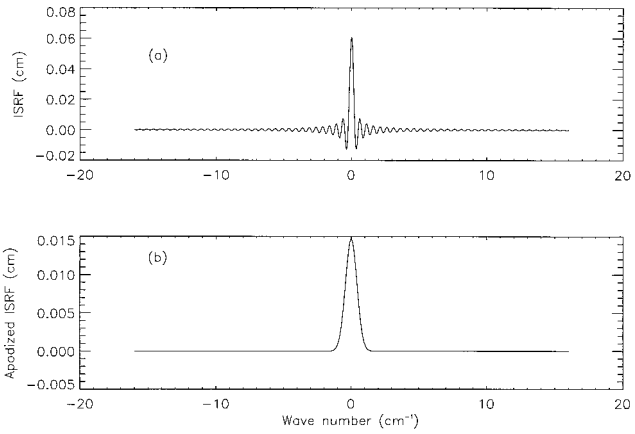

Fig. 1. Nominal IASI instrumental spectral response function (ISRF) for (a) the central wave number $\sigma_0 = 650\ \mathrm{cm}^{-1}$; (b) as in (a) but after apodization with a Gaussian function with half-width at half-height equal to $0.5\ \mathrm{cm}^{-1}$.

3. Application to the Infrared Atmospheric Sounding Interferometer

The IASI will provide spectral measurements of the Earth-atmosphere upwelling radiances in the range from 3.4 to 15.5 μm. The full spectral range is divided into three bands: band 1: 8.26–15.5 μm (645–1210 cm^{-1}); band 2: 4.1–8.26 μm (1210–2450 cm^{-1}); and band 3: 3.6–4.1 μm (2450–2760 cm^{-1}). The nominal sampling interval in the spectral domain will be $\delta\sigma = 0.25\ \mathrm{cm}^{-1}$, which corresponds to a maximum optical path difference of $L = 2$ cm.

For illustrative purposes Fig. 1(a) shows the IASI ISRF corresponding to the central wave number of 650 cm^{-1} (beginning of the first band), whereas Fig. 2(a) shows the IASI ISRF for the central wave number of 2800 cm^{-1}, which corresponds to the end of the third band (e.g., Refs. 12 and 13). The presence of sidelobes for both ISRF's is evident. It is just the presence of these sidelobes that may cause ringing on the spectral features.

For comparison Figs. 1(b) and 2(b) show the convolution product of the two ISRF's above with the Gaussian apodizing function:

$$g(\sigma) = \frac{1}{s\sqrt{2\pi}}\exp\left(-\frac{\sigma^2}{2s^2}\right),$$

where, as in Section 2, σ denotes wave number and s is the usual standard deviation for the Gaussian function. For the convolution product considered

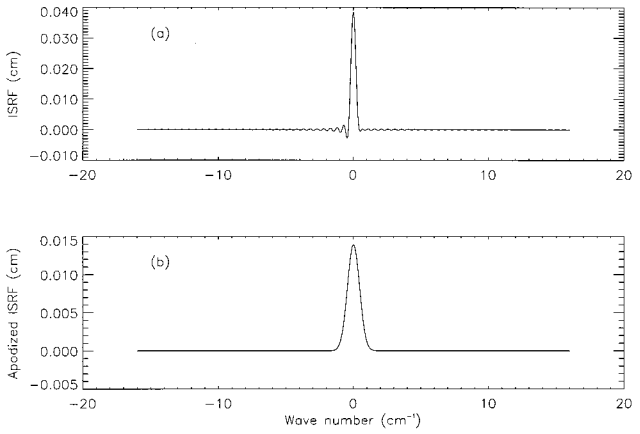

Fig. 2. Nominal IASI ISRF for (a) the central wave number $\sigma_0 = 2800\ \mathrm{cm}^{-1}$; (b) as in (a) but after apodization with a Gaussian function with half-width at half-height $s = 0.5\ \mathrm{cm}^{-1}$.

here, the tuning parameter s has been assigned the value

$$s = \frac{0.5}{\sqrt{2 \log 2}}\ \mathrm{cm}^{-1}, \tag{17}$$

which corresponds to an apodized resolution (half-width at half-height) of $0.5\ \mathrm{cm}^{-1}$. It can easily be seen that the convolution product completely suppresses sidelobes and therefore greatly alleviates the problem of negative transmittances. We will now numerically show that such a product has no effect on the retrieval.

According to our methodology, we need only to compute the Fourier transform G of g and check whether this function introduces a significant truncation below the nominal maximum optical path difference of the IASI, i.e., 2 cm.

The Fourier transform of g is

$$G(x) = \exp(-0.5x^2s^2), \tag{18}$$

which is again a Gaussian function but with parameter $1/s^2$. It is well known that the Gaussian function becomes practically zero after three standard deviations, which for our case corresponds to $3(0.5/\sqrt{2 \log 2})^{-1} \approx 7$ cm, which is much larger than the IASI maximum optical path difference of $L = 2$ cm. Thus we conclude that, with the value of s given by Eq. (17), no effect is to be expected on the retrievals.

The following direct numerical calculation will now definitively support the theoretical ones provided in Section 2. To this end it suffices to show that the matrix (or its inverse)

$$\mathbf{K}^{\mathrm{T}}\mathbf{S}^{-1}\mathbf{K} \tag{19}$$

is equal to the corresponding apodized product

$$\mathbf{K}_a^{\mathrm{T}}\mathbf{S}_a{}^{-1}\mathbf{K}_a. \tag{20}$$

The inverse of matrix (19) or (20) can be thought of as the covariance matrix of the inversions in the case of infinite variances of the background atmospheric state.

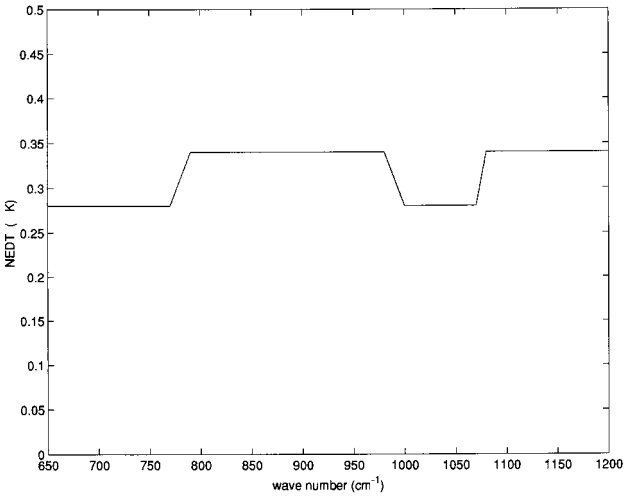

Fig. 3. Expected radiometric noise for IASI band 1. The radiometric noise is expressed in terms of the noise equivalent brightness temperature difference (NEDT) at 280 K.

Since these calculations have primarily an illustrative purpose, for the sake of brevity, we shall limit ourselves to the CO_2 absorption band at 650 cm^{-1}, which is the primary band for temperature sounding. The first IASI band, 645–1210 cm^{-1}, will be used, and only the case of temperature profile retrieval will be considered. The same results apply to different bands and retrieved parameters, e.g., gas constituent profiles. All the computations refer to the tropical model of the atmosphere (Ref. 14).

To compute matrix (19), the following calculations have been performed:

1. With the use of the FASCODE (Ref. 15) radiative transfer code to generate spectral optical depths, the

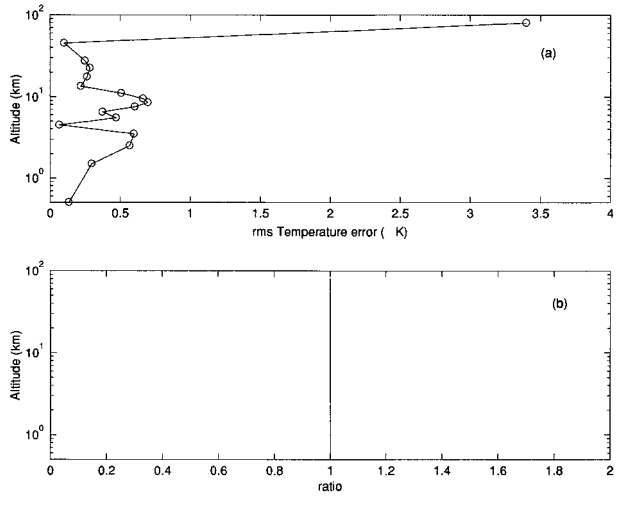

Fig. 4. (a) rms temperature error as a function of altitude corresponding to the case of unapodized radiances (solid curve) and apodized radiances (open circles). The sampling interval is $\delta\sigma = 0.25$. The ratio between the two error curves is plotted in (b).

Jacobian matrix has been computed on the basis of a finite-difference scheme. The Jacobian has then been convolved with the appropriate IASI ISRF (Ref. 12).

2. The covariance matrix of the observations has been assumed diagonal and computed according to the radiometric noise shown in Fig. 3 (Ref. 13).

To obtain the apodized version of matrix (19), the Jacobian obtained at step 1 has been left multiplied by the matrix **O**, with the weights G_i obtained according to Eq. (18). The transformed covariance matrix has been obtained by using Eq. (8).

The square roots of the diagonal terms (rms error) of the inverse of both matrices (19) and (20) are compared in Fig. 4. It is possible to see that no difference between the two sets of values is apparent.

4. Conclusions

In this paper the effect of apodization on the retrieval of geophysical parameters from FTS's has been assessed. Analytical results have been established whose validity hold for any FTS and apodizing function as well. It has been shown that if properly applied, apodization has no effect on retrievals. Furthermore, a general analytical expression for the apodized covariance matrix has been derived. Our mathematical results provide an analytical methodology that may help users of FTS's oriented toward the retrieval problem.

The methodology that we have developed has then been applied to examine the effect of Gaussian apodization on the IASI radiances. The following conclusions can be drawn:

1. A Gaussian apodization that lowers the spectral resolution to 0.5 cm^{-1} greatly suppresses sidelobes present, at an unapodized level, in the IASI ISRF.

2. The above apodization has no effect on retrievals provided that we keep the nominal sampling of 0.25 cm^{-1}.

However, it should be stressed that apodization affects the covariance matrix, which becomes nondiagonal. Since we have to take into account this effect in any retrieval scheme, the practical problem of matrix manipulation could arise. Nondiagonal matrices could heavily affect the speed of computation for the retrievals. The conclusion of our work is, then, that there is no need to apply apodization unless it helps to solve other technical problems.

This paper is dedicated to M. R. Occorsio on his 65th birthday.

This research was supported by the European Organization for Exploitation of Meteorological Satellites under contract EUM/CO/96/407/DD.

References

1. U. Amato, V. Cuomo, and C. Serio, "Assessing the impact of radiometric noise on IASI performances," Int. J. Remote Sensing **16,** 2927–2938 (1995).
2. U. Amato, V. Cuomo, R. Rizzi, and C. Serio, "Evaluating the effect of the inter-relationship among the different spectral bands on IASI performances," Q. J. R. Meteorol. Soc. **123,** 2231–2244 (1997).
3. C. D. Rodgers, "Retrieval of atmospheric temperature and composition from remote measurements of thermal radiation," Rev. Geophys. Space Phys. **14,** 609–624 (1976).
4. A. N. Tikhonov and V. Y. Arsenin, *Solutions of Ill-Posed Problems* (Wiley, New York, 1977).
5. D. W. Marquardt, "An algorithm for least-square estimation of non-linear parameters," J. Soc. Ind. Appl. Math. **11,** 431–441 (1963).
6. C. Serio, U. Amato, and I. De Feis, "Regularization method to solve inverse problems: an investigation in the context of Fourier spectroscopy from satellites," in *Proceedings of the 5th International Workshop on Atmospheric Science from Space Using Fourier Transform Spectrometry* (Central Research Institute of Electrical Power Industry, Tokyo, 1994).
7. F. J. Harris, "On the use of windows for harmonic analysis with the discrete Fourier transform," Proc. IEEE **66,** 51–83 (1978).
8. R. H. Norton and R. Beer, "New apodizing functions for Fourier spectrometry," J. Opt. Soc. Am. **66,** 259–264 (1976).
9. U. Amato, V. Cuomo, and C. Serio, "An advanced optimal spectral estimation algorithm in Fourier spectroscopy with application to remote sensing of the atmosphere," J. Appl. Meteorol. **32,** 1508–1520 (1993).
10. E. A. Robinson and M. T. Silvia, *Digital Foundation of Time Series Analysis* (Holden-Day, San Francisco, Calif., 1981), Vol. 2.
11. R. Beer, *Remote Sensing by Fourier Transform Spectrometry* (Wiley, New York, 1992).
12. F. Cayla, B. Tournier, and P. Hebert, "Performance of new baseline and 9 km option," Rep. IA-TN-0000-5477-CNE (Centre National d'Etudes Spatiales, Paris, 1996).
13. F. Cayla, "IASI level 1 data," Rep. IA-TN-0000-5479-CNE (Centre National d'Etudes Spatiales, Paris, 1996).
14. G. P. Anderson, S. A. Clough, F. X. Kneizys, J. H. Chetwynd, and E. P. Shettle, "AFGL atmospheric constituent profiles (0–120 km)," Rep. ERP 954, AFGL-TR-86-0110 (Air Force Geophysics Laboratory, Hanscom Air Force Base, Mass., 1986).
15. S. A. Clough, F. X. Kneyzys, G. P. Anderson, E. P. Shettle, J. H. Chetwynd, and L. W. Abren, "FASCOD3: spectral simulation," in *Proceedings of the 1988 International Radiation Symposium IRS '88* (Deepak, Hampton, Va., 1989).